



ELSEVIER

Contents lists available at ScienceDirect

Marine Environmental Research

journal homepage: www.elsevier.com



A multidisciplinary analytical framework to delineate spawning areas and quantify larval dispersal in coastal fish

T. Legrand^{a,*}, A. Di Franco^b, E. Ser Giacomi^c, A. Caló^d, V. Rossi^a

^a Mediterranean Institute of Oceanography (UM 110, UMR 7294), CNRS, Aix Marseille Univ., Univ. Toulon, IRD, 13288, Marseille, France

^b Stazione Zoologica "Anton Dohrn", Sede Interdipartimentale di Palermo, Italy

^c Sorbonne Universités (UPMC, Université Paris 06)-CNRS-IRD-MNHN, LOCEAN, 4 Place JUSSIEU, F-75005, PARIS, France

^d Université Côte d'Azur, CNRS, UMR 7035 ECOSEAS, Parc Valrose 28, Avenue Valrose, 06108, Nice, France

ARTICLE INFO

Keywords:

Marine connectivity
Lagrangian flow network
Conservation
Marine protected area
Fish natal origins
Coastal fishes
Mediterranean sea
Ecosystem management
Population dynamics
Models-hydrodynamics

ABSTRACT

Assessing larval dispersal is essential to understand the structure and dynamics of marine populations. However, knowledge about early-life dispersal is sparse, and so is our understanding of the spawning process, perhaps the most obscure component of biphasic life cycles. Indeed, the poorly known species-specific spawning modality and early-life traits, along with the high spatio-temporal variability of the oceanic circulation experienced during larval drift, hamper our ability to properly appraise the realized connectivity of coastal fishes. Here, we propose an analytical framework which combines Lagrangian modeling, network theory, otolith analyses and biogeographical information to pinpoint and characterize larval sources which are then grouped into discrete spawning areas. Such well-delineated sources and their pre-determined settlement sites allow improving the quantitative evaluations of both dispersal scales and connectivity patterns. To illustrate its value, our approach is applied to two case-studies focusing on *D. sargus* and *D. vulgaris* in the Adriatic sea. We evidence robust correlations between otolith geochemistry and modelled spawning areas to assess their relative importance for the larval replenishment of the Apulian coast. Our results show that, contrary to *D. sargus*, *D. vulgaris* larvae originate from both eastern and western Adriatic shorelines. Our findings also suggest that dispersal distances and dispersal surfaces scale differently with the pelagic larval duration. Furthermore, almost 30% of *D. sargus* larvae and 10% of *D. vulgaris* larvae of the Apulian populations come from the Tremiti marine protected area (MPA), exemplifying larval spill-over from MPAs to surrounding unprotected areas. This flexible multidisciplinary framework, which can be adjusted to other coastal fish and oceanic system, exploits the explanatory power of a model tuned and backed-up by observations to provide more reliable scientific basis for the management and conservation of marine ecosystems.

1. Introduction

Dispersal has been identified as a crucial ecological and evolutionary factor which influences demography, population survival, gene flow and local adaptation (Burgess et al., 2016; Lowe et al., 2017). The persistence and dynamics of marine populations are controlled, in addition to local birth and death rates, by connectivity processes (Kool et al., 2013). Connectivity has been defined as the exchange of individuals among geographically separated populations that comprise a metapopulation (Cowen et al., 2006).

Studying dispersal, and more generally the closely-related concept of connectivity, is thus essential to understand population structuring,

a prerequisite for the management and conservation of marine ecosystems. Potential applications of connectivity studies range from informing design of local Marine Protected Areas (MPAs) to replenish fished neighboring areas (Di Franco et al., 2012a; Pelc et al., 2010; Pujolar et al., 2013) and informing maritime spatial planning (Bray et al., 2017; Henry et al., 2018) to improve the design of broad-scale MPAs network and assess their efficiency (Dubois et al., 2016; Rossi et al., 2014).

For coastal fishes, connectivity is assumed to be primarily driven by the dispersion of early-life stages ("propagules") which are transported by ocean currents, a process called "larval dispersal" (Pineda et al., 2007). Indeed, most coastal fishes are characterized by a bipartite life cycle, governing how fish populations structure in space and time. A

* Corresponding author.

Email address: terence.legrand@mio.osupytheas.fr (T. Legrand)

first highly pelagic dispersive phase, encompassing egg and larval stages, is followed by a second relatively sedentary phase as juveniles and adults (Thresher et al., 1989). The transition occurs when individuals take up permanent residence in the demersal habitat, a process named settlement (Levin, 1994), which usually coincides with the metamorphosis of larvae into juveniles (Kingsford, 1988). Then, after a short period, juveniles recruit into the adult fraction of the population (Richards and Lindeman, 1987), which generally constitutes the stages of exploitation and managerial interests.

Even though spawning and subsequent larval dispersal constitute the cornerstones of the fish life cycle, spawning aggregations (areas where fishes gather in high density for the purpose of spawning, Domeier and Colin, 1997) can be massively harvested by fisheries, sometimes inducing collapses in aggregating fish stocks (Sadovy and Domeier, 2005) and ultimately leading to the risk of species extinction (Mitcheson et al., 2013). Furthermore, spawning aggregations can be seen as productivity hotspots of ecological significance since they support both coastal and offshore trophic chains (Fuiman et al., 2015; Heithaus et al., 2008).

As such, scientists and managers should emphasize the focus on spawning areas since their protection leads globally to large benefits for fisheries, ecotourism stakeholders and biological conservation (Erisman et al., 2017). Nevertheless, the precise locations where eggs are spawned are actually one of the main unknown of the fish life-cycle since studies are rarely dedicated entirely at identifying spawning areas (e.g. Calò et al., 2018). The only few spawning sites that have been well documented are situated mainly in tropical reef systems (Domeier and Colin, 1997; Russell et al., 2014), perhaps where connectivity studies are facilitated by the relatively small-size and closeness of the seascape. It contrasts with the openness and continuous coastlines of temperate systems, such as the Mediterranean Sea, where spawning areas are largely unknown. In addition, while knowledge about fish home range exists (Di Franco et al., 2018), the way it is usually defined disregards the reproductive movements, despite observational evidence that many coastal fishes move offshore during the spawning season (Aspillaga et al., 2016; Giacalone et al., 2018).

In a context of anthropogenic and environmental perturbations (Ciannelli et al., 2013), a major challenge is thus to provide scientifically-based information about spawning areas in all oceanic systems to achieve a sound spatial management and protection of coastal fishes. However, this objective has been hampered by the complexity of fish life-cycles, the paucity and disparity of observational records and the absence of a unifying methodology to do so.

In this context, a possible approach to investigate the location of fish spawning could be based on the scientific information on larval dispersal, coming from multiple methodologies. Many methods, each with its own strengths and weaknesses, have been used to investigate the ins and outs of larval dispersal (Calò et al., 2013). They are principally divided into four categories: study of marine larvae, artificial tags, natural tags (genetics, otolith sclerochronology, otolith geochemical analyses) and numerical modelling (physical or bio-physical, Nolasco et al., 2018). To increase the accuracy of larval dispersal analyses, it seems fundamental to use a combination of complementary methodologies, maximizing the strengths of each technique. However, while the proportion of works that mixed different methodologies is currently growing, only few studies have used at least two methods to characterize larval dispersal, with a preferential combination of numerical biophysical models with genetic markers and/or otoliths analysis (Nolasco et al., 2018).

Most of these multi-disciplinary studies aimed to locate the potential destinations of propagules by means of forward-in-time advection from pre-determined hypothesized sources, such as MPAs or sampling sites (Bray et al., 2017; Carlson et al., 2016; Di Franco et al., 2012a; Melià et al., 2016; Pujolar et al., 2013). Di Franco et al. (2012b, 2015)

have investigated connectivity for two coastal fish species using otolith techniques; their results set the lower limits of dispersal and distinguish several natal origins for both fishes, but there was little information about regional connectivity patterns and no indication at all of the extension and localization of these natal regions.

In this paper, we propose a flexible analytical framework to delineate and characterize fish spawning areas by integrating model simulations and information from otolith studies. We test our framework by exploiting two data-rich case-studies focusing on the coastal fishes *Diplodus sargus sargus* (Linnaeus, 1758) and *Diplodus vulgaris* (Geoffrey Saint Hilaire, 1817) in the Adriatic sea.

2. Materials and methods

2.1. General description

Our analytical framework consists of dissecting the main steps of dispersal, namely the “origins”, the “transport” process and the “destinations”, backward-in-time. A Lagrangian bio-physical model, parameterized with adequate numerical choices and early-life traits of the target species obtained from biological knowledge (including otolith sclerochronology data), is used to assess “transport” (“Lagrangian Flow Network” box in Fig. 1). “Destinations” are pre-determined by the locations where juveniles were sampled for the otolith studies. One of the main novelty is to consider the whole oceanic domain of interest as a mosaic of potential larval sources (putative “origins”). These are refined step-wise by biological knowledge (including otolith geochemical data) of our target species (“Filtering” box in Fig. 1). It allows us to assess larval dispersal scales (“Scales of dispersion” box in Fig. 1) in a robust manner thanks to millions of simulated larval trajectories. Adequate statistical normalizations allow computing the proportion of each source to the total larval pool supplied into pre-determined destinations (“Diagnosing” box in Fig. 1). These probabilities are then exploited to quantitatively assess the connectivity induced by larval dispersal (“Patterns and magnitude of connectivity” box in Fig. 1). Then, by incorporating additional ecological and connectivity knowledge, we fit simulated larval sources with otolith geochemistry to better locate and evaluate the relative importance of discrete spawning areas (“Localization & characterization of spawning areas” box in Fig. 1) for the replenishment of the sampled settlement sites.

2.2. Lagrangian Flow Network: tuning parameters and computing

The Lagrangian Flow Network (LFN) methodology combines network theory tools and particle-tracking modelling to investigate transport and dispersal processes in oceanic flows. As any off-line particle tracking model, it can be coupled to all gridded two- or three-dimensional velocity fields available, returning dispersal diagnostics as realistic as the input flow field. Full description can be found in Rossi et al. (2014); Ser-Giacomi et al. (2015a, b) and Dubois et al. (2016). Here, the LFN is used to simulate the dispersal of passively drifting larvae as horizontal Lagrangian trajectories obtained through the integration of a realistic regional flow field.

The ad-hoc LFN configuration is obtained by selecting the most adequate hydrodynamical model and thanks to the fine-tuning of seven LFN parameters (“Parameters tuning” box in Fig. 1) in accord with both biological (including the information derived from the otolith analyses) and numerical knowledge from the scientific literature. Only the most relevant elements are summarized hereafter (see SI A-1.1 for further information). The starting date of each numerical experiment e is simulating a single spawning event while the ensemble of Lagrangian experiments E has to cover the full range of spawning dates obtained from otolith sclerochronology. Tracking time is set to mimic the Pelagic Larval Duration (PLD; i.e the time larvae spend in plankton),

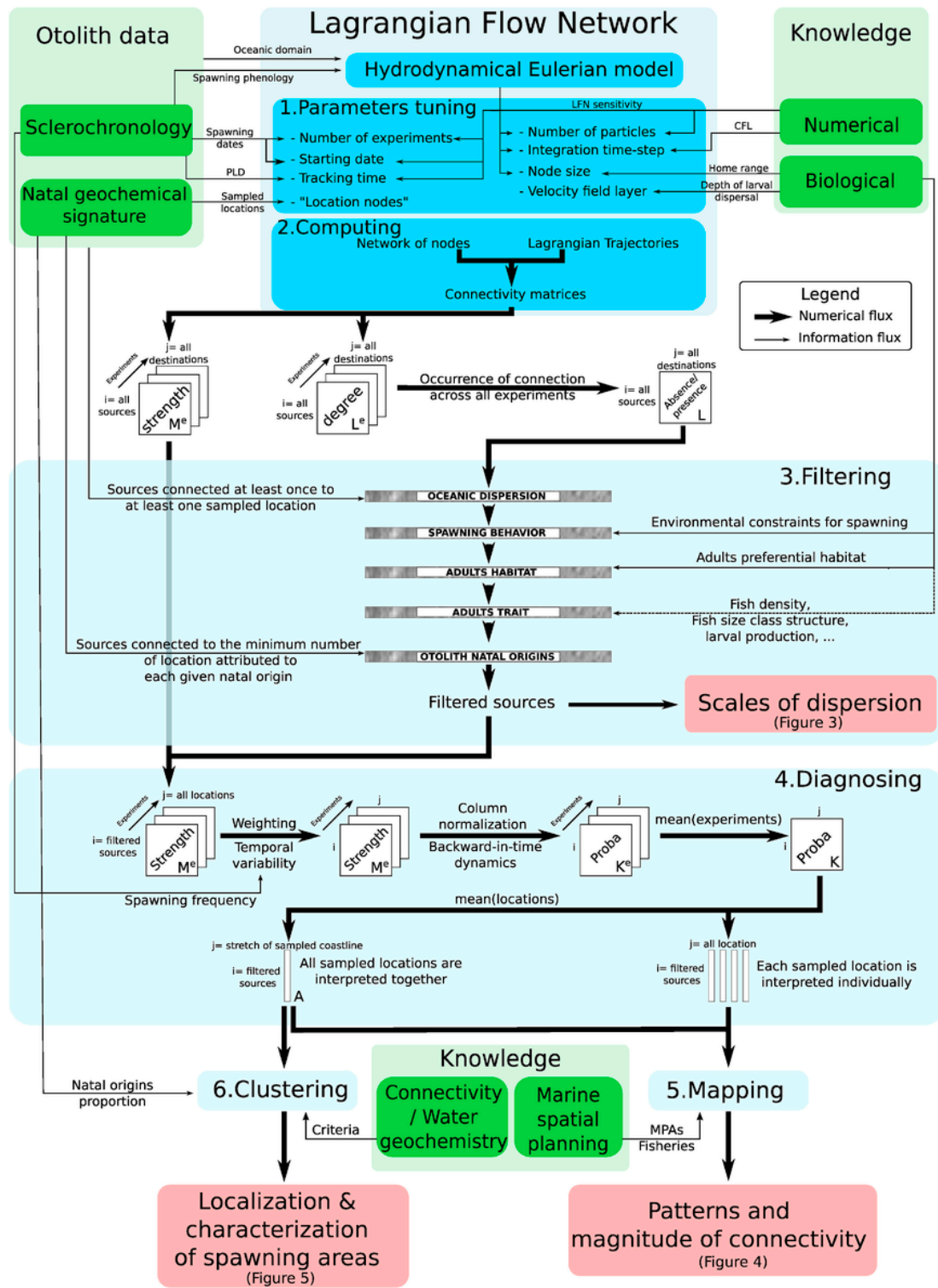


Fig. 1. Schematic representation of our integrative framework which combines Lagrangian modelling and expert knowledge (including otolith analyses) in order (i) to investigate the scales of dispersion, (ii) to determine the patterns and magnitude of connectivity and (iii) to locate and characterize spawning areas for conservation purposes. Our framework is structured according to the color code: blue annotations refer to the numerical methodologies, green annotations symbolize expert knowledge (from existing bibliography) and red boxes highlight the key results. PLD stands for Pelagic Larval Duration and CFL for Courant-Friedrichs-Lewy (see section 2.2) for a definition of all the terms used). (For interpretation of the references to color in this figure legend, the reader is referred to the Web version of this article.)

which is also estimated from otoliths sclerochronology. The network of nodes (i.e. sub-areas of the discretized oceanic domain) resolution is adjustable, compromising both the level of analyses and the computation time. It must be at least twice larger than the spatial resolution of the velocity field given by the hydrodynamical model. Note that each

node has the same area and contains the same initial number of particles. The number of particles per node should be larger or equal to 100 particles, as prescribed by Monroy et al. (2017) and the Runge-Kutta time step should fulfill the Courant-Friedrichs-Lewy (CFL) condition imposed by the velocity field itself (Courant et al., 1928). The vertical

layer of the velocity field (for z-coordinates model) must be chosen according to the most probable depth at which larvae of the target species are more likely to be found. Note that our Lagrangian trajectories are currently 2-dimensional, without considering any larval diel migration. For each settlement sites (i.e. where juveniles were sampled in otolith studies), we attributed one or more *location nodes* in the close vicinity of each sampled *location*.

After computing hundreds of million Lagrangian trajectories and recording the initial and final positions of each particle, a connectivity matrix of particles is built similarly for each numerical experiment $e \in [1; E]$ ("Computing" box in Fig. 1, see SI A-1.2 for further information). We saved an ensemble of E connectivity matrices, which have as many rows and columns as the total number of nodes N in the network and which contain all information about dispersal. Each matrix element $i-j$ characterizes the connection between the origin node $i \in [1, N]$ and the destination node $j \in [1, N]$ from a given starting date and during a fixed tracking time.

The connection between any pairs of nodes can be characterized at two levels: the binary link (presence/absence of connection, L^e matrices) and the weights of the link (the number of transported particles associated to all existing link, M^e matrices Ser-Giacomi et al., 2017). The binary links, i.e. L^e matrices, are used to successively filter-out the putative origin nodes in order to locate the effective sources of larvae (see section 2.3). The associated weights, i.e. M^e matrices, are used to compute probabilities of larval emission from the effective sources to the surveyed locations (see section 2.4).

2.3. Filtering

We aim at determining the most relevant sources, among all the putative origins, of the larvae whose trajectories ended in the pre-determined *location nodes* ("Filtering" box in Fig. 1). The effective sources of larvae are investigated by applying successively restrictive filters over the full set of potential origin sources, sequentially refining our characterization. The flexibility of our framework allows us to add or skip any given filter depending on the level of knowledge of the studied species and on the confidence to be attributed to each piece of information. It implies that the more information we have about the biological traits of the studied species ("Biological knowledge" and "otolith data" boxes in Fig. 1), the more precise and realistic are the final larval sources. Different filtering layers are defined hereafter and subsequently applied to the suite of connectivity matrices:

- Among all potential sources (i.e. all nodes), the first filter selects those which are connected, at least once over all experiments (i.e. over all spawning events) to at least one out of all sampling locations (i.e. one of all *location nodes*). Note that this first filter, based only on the cumulative binary matrix L , is a strong constraint imposed by the geographical extent of the otoliths sampling area. When mapping those selected nodes, it gives us the maximal and theoretical extent of all sources (see SI A-2 for further information).
- The second step filters in all putative sources that are favorable for spawning based on the best available knowledge concerning spawning behavior of the studied fish. This could be derived from any environmental criteria triggering spawning (e.g. threshold of temperature, light, etc) or any constraint restricting spawning (e.g. bathymetric limit, see section 2.6.3).
- The third step filters in all putative sources whose environmental characteristics are suitable for adults (e.g. preferential habitats). Indeed, the overall contribution of adults to broad-scale dispersal can be reasonably neglected since these stages are rather territorial, especially littoral fishes that show strong site fidelity (Di Franco et al., 2018).

- One may add as many additional filters as possible to further refine the characterization of the putative larval sources. These extra filters must be spatialized dataset derived from the finest biological knowledge of the target species. For instance, spatial information about fish density, sex-ratio and size class structure, which, in combination with a female size/eggs production relationship (Marshall et al., 2019), could further constrain the initial larval production of each source node.
- The last filter selects those larval sources whose downstream connections (e.g. forward-in-time dispersal) are concordant with the diversity of origins revealed by otolith geochemistry. In other words, larval sources must send larvae to at least the minimal number of sampled location successfully replenished by the less-ubiquitous fish natal origins, as assessed from otolith geochemical analyses.

After the superposition of all filters, the remaining "origin" nodes are the most likely larval sources in the domain.

2.4. Diagnosing

The filtered larval sources are analyzed from the weighted connectivity matrices M^e to quantitatively characterize, as explained hereafter, the probabilities of connection with all sampling locations ("Diagnosing" box in Fig. 1, see SI A-3 for further information).

First, to take heed of the temporal heterogeneity of spawning, our ensemble of experiments E must simulate the observed spawning variability. This is achieved by defining a new matrix \overline{M}^e for each experiment which modulates each original connectivity matrix M^e , representing one spawning event, with a weight p^e prescribed by its corresponding spawning dates frequency obtained from the otolith analyses.

To be interpreted as probabilities, connectivity matrices of particles must be normalized. When looking for the probabilities of connection from *location node* j to filtered source node i , we approximate backward-in-time dynamics by a column-normalization of each connectivity matrix, even though it has been originally computed forward-in-time (Ser-Giacomi et al., 2015a, b). These backward-in-time "upstream" probabilities are interpreted as follows: if we randomly select a particle settled in any *location node* j after the tracking time (PLD), this particle has a probability $\in [0,1]$ to originate from node i . Therefore, this probability measures the relative contribution of that source node i to the total pool of larvae sent by all sources which successfully settled in *location node* j . The numerical experiments are merged together by averaging all E connectivity matrices into one final probabilistic matrix denoted as K which summarizes all the relevant connectivity information. By selecting in this final matrix K the row i , corresponding to the index of any filtered sources, and the column j , corresponding to the indices of all *location nodes*, one can investigate the probability of connection for all existing pairs of source node and *location node*. In addition, one can consider all *location nodes* together by averaging the probabilities of their corresponding nodes (column indexed j) into one vector called A . Here we mainly exploit this configuration as it allows to take a global perspective of the surveyed area, which is compatible with the next clustering step.

2.5. Clustering

Besides the characterization of larval sources described in previous section 2.4, our final objective is to pinpoint spawning areas in our simulations as constrained by the results of otolith geochemistry. As such, once the most relevant *source* have been selected through the successive filters and their transport probabilities characterized ("Mapping" box in Fig. 1), we aim here at grouping these *source* several regional clusters whose relative contributions for supplying larvae to the surveyed locations would match the natal origins revealed by

otolith geochemistry (“Clustering” box in Fig. 1). Determining pertinent criteria and numerical algorithm for clustering is not a trivial issue (e.g. Fortunato, 2010; Rossi et al., 2014; Ser-Giacomi et al., 2015a). We retain here five criteria which are based on empirical and published knowledge that are used to gather the full set of source nodes into several clusters as follows:

- The number of cluster must be equal to the number of natal origins deduced from otolith geochemical analyses.
- Each cluster must be composed of geographically contiguous or almost contiguous source nodes, fulfilling the assumption that seawater geochemistry is homogeneous at small-scale (e.g. within a given water mass).
- Each cluster should have a maximal extension of about 400 km since it is the typical length-scale at which the geochemical composition of seawater is supposed to vary substantially, hence conferring distinct geochemical signatures in otoliths (Gibb et al., 2017).
- Any relevant connectivity information about the spatial differentiation of fish population must be considered in the cluster delimitation (e.g. through genetics, tagging and tracking techniques; Calò et al., 2013).
- The precise delimitation of each simulated cluster can be further refined by considering the observed proportions of natal origins derived from otolith geochemistry. In other words, the fine-tuning of the clusters' boundaries must be done while maximizing the correlation between natal origin proportions and the aggregated probabilities of larval sources.

2.6. Case-studies

We exploit two data-rich case-studies to test our framework and its effectiveness for locating spawning areas and for evaluating connectivity patterns of both *Diplodus sargus* and *Diplodus vulgaris* in the Adriatic Sea (Fig. 2)

2.6.1. Oceanic domain and hydrodynamical model

The Eulerian gridded velocity field comes from the high-resolution ($\frac{1}{45}^\circ$) Adriatic-Ionian REgional configuration (AIREG, Ciliberti et al., 2015; Oddo et al., 2006), which is based on the NEMO kernel (Madec and others, 2015) and has been developed by the CMCC Ocean Lab (Fig. 2a, see SI B-1 for further information).

2.6.2. Otolith data

Post-settlers (i.e. 1–1.5 cm body length) of *D. sargus* and *D. vulgaris* were collected at seven distinct sampled locations separated by 10–30 km, corresponding to about 180 km stretch of the Apulian coast (Fig. 2b; Di Franco and Guidetti, 2011; Di Franco et al., 2013, 2012b, 2015). Data gathered from otolith sclerochronology (Di Franco and Guidetti, 2011; Di Franco et al., 2013) and geochemical analysis (Di Franco et al., 2012b, 2015) are reported in Table 1 (see SI B-3.1).

2.6.3. Biological traits

Knowledge of biological traits is generally sparse and uncertain for most fish species. Concerning our case-studies, quite reliable information is however available for both studied species. Recent reports of the depths at which *D. sargus* and *D. vulgaris* commonly spawn range be-

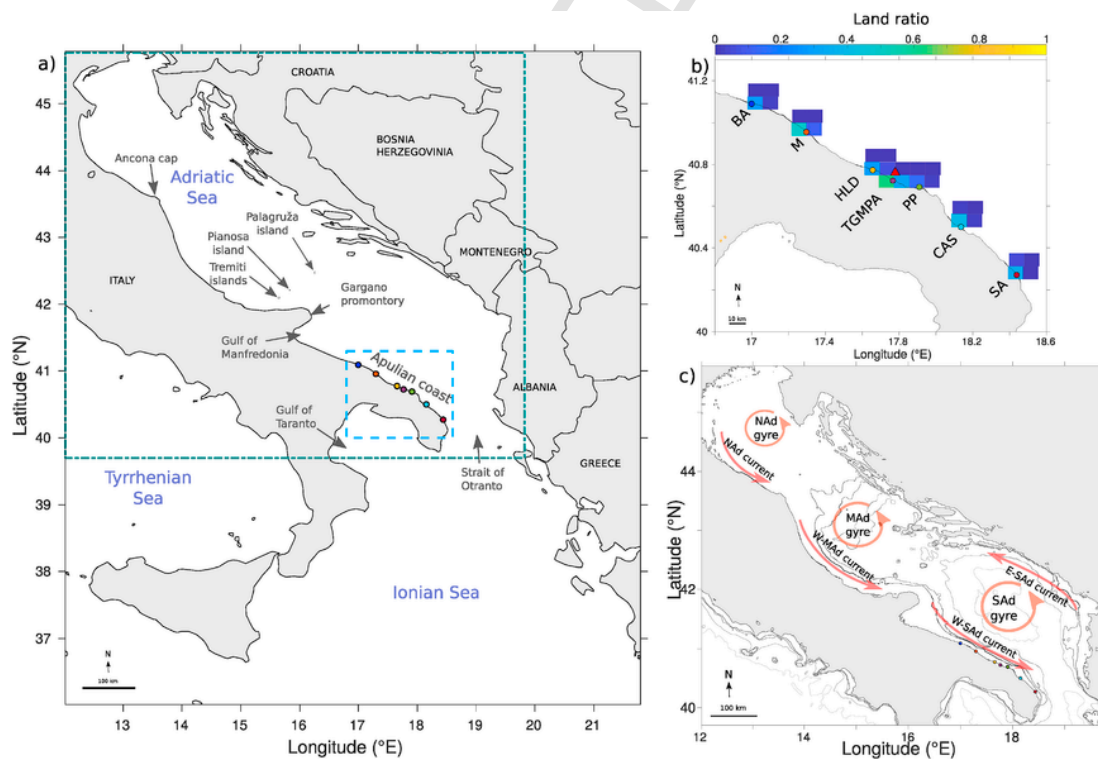


Fig. 2. Geographical location, topography and schematic circulation of the study area. Panel a) displays the network domain ($36^\circ - 46^\circ \text{N}$, $12^\circ \text{E} - 22^\circ \text{E}$). Panel b) discloses a zoom over the Apulian coast and indicates the seven locations (colored dots) named, from north to south: Bari (BA), Monopoli (M), Hotel La Darsena (HLD), Torre Guaceto Marine Protected Area (TGMPA), Punta Penna (PP), Casalabate (CAS) and San Andrea (SA). Location nodes, associated with each sampling location, are colored according to their land ratio (see SI A-1.1). The red triangle corresponds to the barycenter of all location nodes centers. Panel c) presents a schematized view of the mean surface circulation of the Adriatic Sea (red arrows). The system is dominated by the Western South Adriatic (W-SAd) current, the Eastern South Adriatic (E-SAd) current, the Western Middle Adriatic (W-MAd) current, the Northern Adriatic (NAd) current, the South Adriatic (SAd) gyre, the Middle Adriatic (MAd) gyre and the North Adriatic (NAd) gyre (adapted from Artegiani et al., 1997b; Millot and Taupier-Letage, 2005). The thin grey lines in panel c) corresponds to isobaths 80 m, 100 m, 200 m and 1000 m, respectively. (For interpretation of the references to color in this figure legend, the reader is referred to the Web version of this article.)

Table 1

Summarized information and early-life traits gathered for *D. sargus* (Di Franco and Guidetti, 2011; Di Franco et al., 2012b) and *D. vulgaris* (Di Franco et al., 2015), as obtained from sclerochronology and geochemical analyses of their otoliths.

Early-life traits	Species	
	<i>D. sargus</i>	<i>D. vulgaris</i>
Number of samples	140	160
Spawning duration	04/05/2009–24/05/2009	20/10/2009–14/02/2010
Median PLD (days)	17 ± 1	47 ± 8
Number of natal origins	3	7

tween 0 and 80 m deep (Aspillaga et al., 2016; Giacalone et al., 2018). Moreover, larvae of *D. sargus* in the field have been mainly observed at around 10 m depth (Olivar and Sabatés, 1997). Both species have similar adult sedentary behavior, with individuals home ranges that are typically smaller or equal to 1 km² (Alós et al., 2012; Di Lorenzo et al., 2014; Di Franco et al., 2018). Concerning the preferential habitat of adults, *D. sargus* and *D. vulgaris* inhabit coastal rocky reefs, *Posidonia oceanica* meadows and coralligenous formations (Guidetti, 2000; Harmelin-Vivien et al., 1995; Lenfant and Planes, 1996).

Table 2

Summary of specie-specific numerical parameters (and their corresponding early-life traits) for *D. sargus* and *D. vulgaris*. The common parameters are a node size of 1/16°, the selected vertical layer of the flow at 10 m deep, a Runge-Kutta time step of 20 min and an initialization of 900 particles per node.

Numerical parameters	Species	
	<i>D. sargus</i>	<i>D. vulgaris</i>
Range of starting dates	04/05/2009–24/05/2009	05/11/2009–28/01/2010
(spawning duration)		
Starting dates subsampling (days)	1	4
(spawning periodicity)		
Tracking time (days) (PLD)	17	47
Number of experiments (spawning events)	21	22

High-resolution maps of these fish preferential habitats over the whole Adriatic were obtained from seabed habitat maps downloaded on the EMODnet portal. They were then hand-corrected using 2-steps procedures (see SI B-3.2). To our knowledge, this improved map represents perhaps the best and most updated geo-referenced seafloor cartography for the Adriatic Sea.

2.6.4. Tuning model parameters from published knowledge

Biological information derived from otolith analyses and literature review on biological traits for *D. sargus* and *D. vulgaris* are used to fine-tune the LFN parameters introduced in section 2.2 (see SI B-4). The parameters retained for this case-study are reported in Table 2. For each connectivity matrix, the LFN model builds a network of around 10000 quasi-rectangular oceanic nodes of $\frac{1}{16}^\circ$ side (that is about 7 km) and computes around 9 million trajectories. In total, about 380 million of particles trajectories were calculated to produce 43 high-resolution connectivity matrices for both species.

3. Results

3.1. Scales of dispersion

The first filter returns the maximal and theoretical extent of all the larval sources, as constrained by the oceanic circulation experienced during larval drift. For *D. sargus*, filter-1 larval sources spread from 43.2°N to 40.2°N along the Italian coast (Fig. 3a). Median dispersal distance is 175 km, maximal dispersal distance is 355 km and the “backward” dispersal plume surface is 35662 km² (see Tables 3 and SI B-5). For *D. vulgaris*, putative larval sources extend from 44.2°N to 36°N in almost all the Adriatic Sea and the northern Ionian Sea (Fig. 3b). The maximal dispersal distance median is 1.7 times higher than *D. sargus*'s one whereas the median distance is quite similar (ratio of 1.0). The dispersal plume surface is 233199 km², around 6.5 times larger than *D. sargus*'s one (Table 3).

The second filter selects all larval sources whose environmental characteristics fulfill the favorable conditions for spawning to occur. Here it is a “coarse” bathymetric filter selecting all nodes whose depths range 0–80 m, that is the depths at which *D. sargus* and *D. vulgaris* commonly spawn (see section 2.6.3). For *D. sargus*, filter-2 larval sources extend from 43.2°N to 40.2° along the Italian coastline (Fig. 3a). The

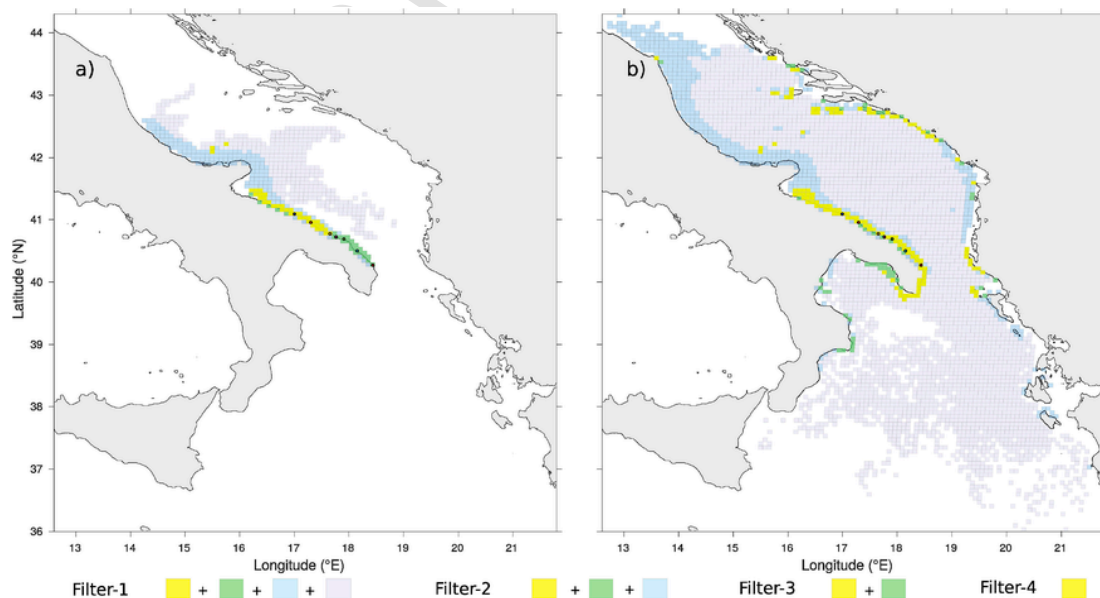


Fig. 3. Spatial scales of dispersion as given by the characterization of larval sources by successive filtering procedure for *D. sargus* (panel a) and *D. vulgaris* (panel b).

Table 3

Quantitative evaluation of the dispersal scales of *D. sargus* and *D. vulgaris* for each filter successively applied. Median/maximal dispersal distance corresponds, respectively, to the median/longest distance measured between all source nodes and the barycenter of the seven sampled locations (see SI B-5). The dispersal plume surface corresponds to the total surface of all nodes acting as putative larval sources.

Species	Quantitative diagnostics	Filter-1	Filter-2	Filter-3	Filter-4
<i>D. sargus</i>	Median dispersal distance (km)	175	185	135	135
	Maximal dispersal distance (km)	355	355	245	245
	dispersal plume surface (km ²)	35662	12918	3700	2183
<i>D. vulgaris</i>	Median dispersal distance (km)	170	210	90	90
	Maximal dispersal distance (km)	590	550	470	470
	dispersal plume surface (km ²)	233199	41606	11160	7884

dispersal plume surface is 12918 km², which corresponds to a reduction of the filter-1 plume by about 64% (Table 3). For *D. vulgaris*, sources spread from 44.2 °N to 37.2 °N (Fig. 3b). The dispersal plume surface is 41606 km², indicating a reduction by 82% from filter-1 plume (Table 3). Median and maximal dispersal distances as well as dispersal plume surface are higher for *D. vulgaris* than for *D. sargus*, with a ratio of 1.1, 1.5 and 3.2, respectively (Table 3).

The third filter display all larval sources which house adults preferential habitats, that is rocky reefs, *Posidonia oceanica* meadows and coralligenous formations in our case-studies (see section 2.6.3). For *D. sargus*, filter-3 larval sources extend from 42.2 °N to 40.2 °N (Fig. 3a). The dispersal plume surface is 3700 km², corresponding to a reduction by 71% of the filter-2 surface (Table 3). For *D. vulgaris*, larval sources expand from 43.6 °N to 38.5 °N (Fig. 3b). The dispersal plume surface is 11160 km², implying a reduction by 73% of the filter-2 surface (Table 3). The maximal dispersal distance and the dispersal plume of *D. vulgaris* are respectively 1.9 and 3.0 times higher than those of *D. sargus*. The median dispersal distance for *D. sargus* is 1.5 higher than for *D. vulgaris* (Table 3).

The fourth filter selects the larval sources which are connected to the minimum number of sampled locations successfully replenished by the less-ubiquitous fish natal origins, as assessed from otolith geochem-

ical analyses. In other words, the fourth filter selects the larval sources which send larvae to at least “x” different sampled locations, “x” being determined by the minimum number of sampled locations in which the rarest fish natal origins was found. Here, “x” is four for *D. sargus* and three for *D. vulgaris* (see SI B-3.1). In our case-studies, this last filter provides the most refined sources which take into account all constraints imposed by realistic oceanic dispersal as well as observation-based biological knowledge. For *D. sargus*, filter-4 larval sources expand from 42.2 °N to 40.8 °N (Fig. 3a), located especially along the Apulian coast and around the Tremiti archipelago (composed of the main island and the isolated Pianosa islet; see Fig. 2a). The dispersal plume surface is now 2183 km², that is a reduction by 41% of the filter-3 plume (Table 3). For *D. vulgaris* sources spread from 43.6 °N to 39.6 °N on both Adriatic shores. Note that some sources are located within the gulf of Taranto and one noticeable larval source remains in the middle of the Adriatic Sea, next to the Palegruza island at 42, 5 °N, 16, 4 °E (Fig. 3b). The dispersal plume surface is 7884 km², corresponding to a reduction by 29% of the filter-3 plume. The maximal dispersal distance and the dispersal plume of *D. vulgaris* are higher than those of *D. sargus*, with a ratio of 1.9 and 3.6, respectively. The median dispersal distance for *D. sargus* is 1.5 higher than for *D. vulgaris*.

Altogether, the superposition of the four filters has reduced the dispersal plume surface by 94% for *D. sargus* and by 97% for *D. vulgaris*. When comparing three quantitative dispersal diagnostics between both species, the mean ratios of *D. vulgaris* to *D. sargus* are 0.9 ± 0.2 for median distances, 1.7 ± 0.2 for maximum distances and 4.1 ± 1.6 for dispersal surfaces (Table 3).

3.2. Patterns and magnitude of connectivity

The flexibility of our approach allows us to map and analyze the probabilities of all source nodes, i.e. the probability that larvae whose dispersal ended up in one of the seven sampled locations originated from that source node, for each levels of filtering. We chose here to exploit mainly the most constrained larval sources returned by the superposition of the four filters (Fig. 4, see SI B-6 for the other filters). Note that this larval source probability are integrated here as the larval source's spawning potential. For *D. sargus*, the core larval sources are located along the Apulian coast and around the Tremiti archipelago. Sources situated next to the main islands of the Tremiti archipelago are characterized by high probabilities, i.e. spawning potential (0.1). The

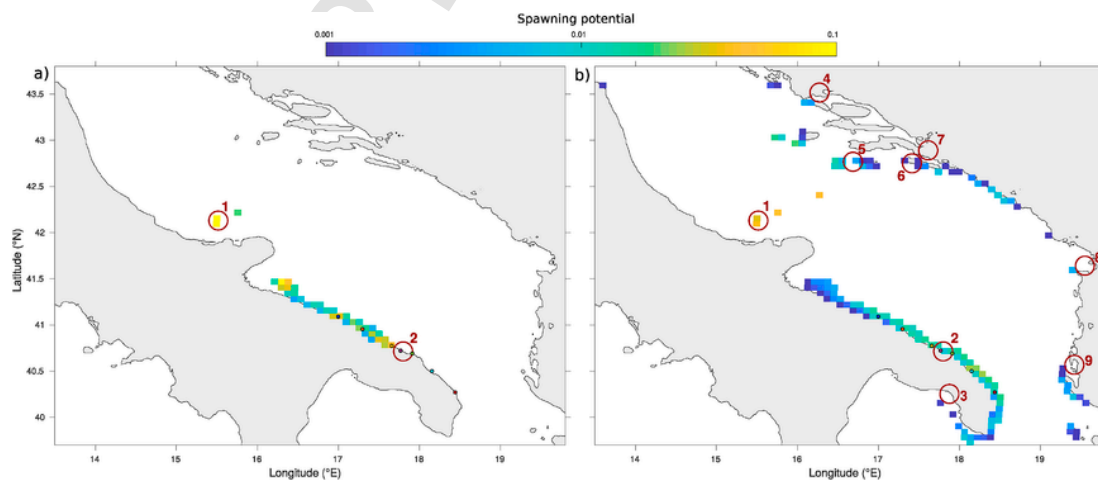


Fig. 4. Quantitative patterns of connectivity for *D. sargus* (panel a) and for *D. vulgaris* (panel b): maps of the most constrained larval sources (after applying the superposition of the four filters), along with their associated probabilities (the probability of that node to supply larvae to the surveyed stretch of Apulian coastline) which are integrated here as the larval source's spawning potential. Red circles represent the current Marine Protected Areas (MPAs) which have connection with the sampled locations: (1) Tremiti islands, (2) Torre Guaceto, (3) Porto Cesaro, (4) Pantana, (5) Lastovo archipelago, (6) Mljet, (7) Mali Ston Bay, (8) Lumi Buna-Velipoje and (9) Karaburun-Sazani Island (see SI B-7). (For interpretation of the references to color in this figure legend, the reader is referred to the Web version of this article.)

other isolated source located next to the isolated Pianosa island has moderate spawning potential (~ 0.01). Sources along the Apulian coast are characterized by a wide range of spawning potential spanning 0.001–0.1. Three locals maximal, with spawning potential ranging from 0.01 to 0.1, can be distinguished at around 41.5 °N, 41.1 °N and 40.7 °N. The other sources have moderate to low spawning potential of the order of 0.001–0.01. For *D. vulgaris*, the core larval sources are located from 43.6 °N to 39.6 °N on both Adriatic shores (see section 3.1). Most probable sources (spawning potential of 0.1) are around the Tremiti archipelago and the Palagruža island (42 °N, 17 °E). Sources of intermediate spawning potential (~ 0.01) are found along the Apulian coast (from 41.2 °N to 40.2 °N), on the eastern part of the gulf of

Taranto (around 18 °E), next to the Croatian islands (from 43 °N to 42.5 °N), along the southern Croatian coastlines (42.3 °N), and along both northern (41.5 °N) and southern Albanian coastlines (40.2 °N). The remaining sources, i.e. near Ancona cape (43.5 °N, 13.8 °E) and along the northern Apulian coast, are associated to low spawning potential (~ 0.001).

We next analyze, for both species, the strengths of the existing connections between MPAs and the sampled locations. It is equivalent to assess the proportions of larvae supplied by the local MPA network to the sampled locations (Fig. 4, see SI B-7). Our model simulations suggest that two MPAs for *D. sargus* (Fig. 4a) and nine MPAs for *D. vulgaris* (Fig. 4b) are supplying larvae to the sampled locations. The spawning potential associated to each MPA, interpreted here as proportions of the total pool of larvae supplied to the sampled locations, are documented in Table 4. Tremiti MPA emerges as the most important larval supplier, providing 26,4% of *D. sargus* larvae and 7,5% of *D. vulgaris* larvae settled along this stretch of Apulian coastline. By summing up probabilities, the total contribution of the local network of MPAs to the total pool of larvae settled in the sampled locations is about 30% for *D. sargus* and 24% for *D. vulgaris*.

Table 4

MPAs associated proportions for *D. sargus* and *D. vulgaris*, indicative of their relative contribution in the total larval pool supplied to the sampled stretch of Apulian coastline. Note that the proportions of larvae supplied by each MPA into each location is given in SI B-7.

MPAS		Species (%)	
Index	Name	<i>D. sargus</i>	<i>D. vulgaris</i>
1	Tremiti islands	26.4	7.5
2	Torre Guaceto	4.4	7.5
3	Porto Cesaro	–	0.1
4	Pantana	–	0.9
5	Lastovo archipelago	–	5.6
6	Mljet	–	0.5
7	Mali Ston Bay	–	0.4
8	Lumi Buna-Velipoje	–	0.5
9	Karaburun-Sazani Island	–	0.6
–	All	30.8	23.6

3.3. Localization and characterization of spawning areas

To pinpoint the most robust and realistic spawning areas, we exploit the flexibility and statistical power of the LFN model while we constrain the grouping procedure to match the natal origins revealed by otolith geochemistry. Using criteria defined in section 2.5, filter-4 larval sources are grouped into three and seven clusters (e.g. “coherent spawning regions”) for *D. sargus* and for *D. vulgaris*, respectively (Fig. 5a and b). For both species, one cluster embraces the larval sources

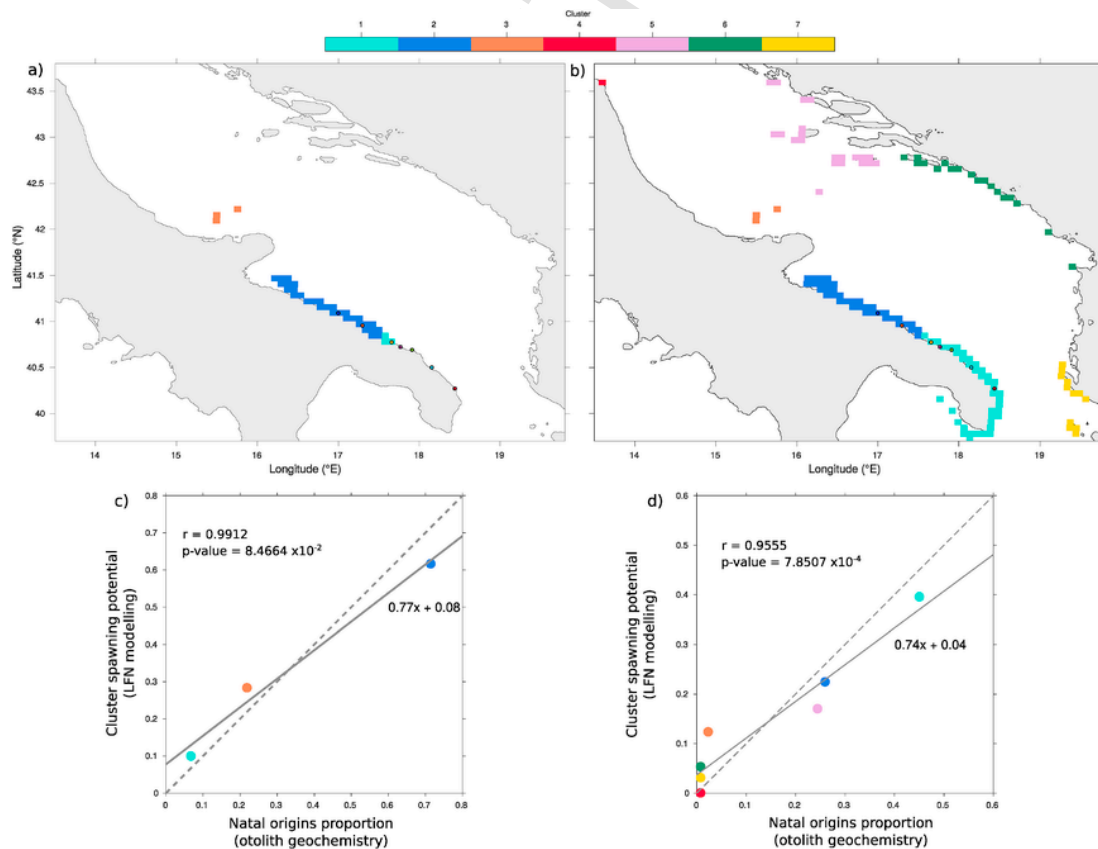


Fig. 5. Spawning areas geographically-delimited thanks to criteria defined in section 2.5 and characterization of their relative contributions to the total pool of larvae settled in the Apulian coast. Clusters of the most constrained larval sources (panels a, b) and correlations between simulated larval contributions and observed natal origin proportions (panels c, d) for *D. sargus* (panels a, c) and *D. vulgaris* (panels b, d).

around the Tremiti archipelago while the sources located along the Apulian coast are separated into two clusters by a boundary that we imposed to both species. Indeed, this boundary was fixed for *D. sargus* by following the last clustering criterion (that is to maximize the fit between model estimations and otolith geochemical analyses, see SI B-8); the same boundary is then used for *D. vulgaris* assuming water geochemistry background is the same for both species. Concerning the four other spawning areas of *D. vulgaris*, one cluster corresponds to the northernmost source located next to Ancona cap and three other clusters represent subgroups of all the source nodes spread along the eastern shores.

We report the relative larval supply proportions attributed to each cluster by summing up the probabilities, i.e. spawning potential, of all the source nodes pertaining to a given cluster. For *D. sargus*, cluster 2 is characterized by the highest spawning potential (0.61), cluster 3 has intermediate spawning potential of 0.29 and cluster 1 exhibits the lowest contribution (0.1; Fig. 5a,c). For *D. vulgaris*, cluster 1 has the highest spawning potential (0.4) whereas clusters 4, 6 and 7 are characterized by the lowest spawning potential (> 0.01 , 0.05, 0.03, respectively). Clusters 2, 3 and 5 have moderate contributions of 0.23, 0.12 and 0.17, respectively (Fig. 5b,d).

We analyze the correlations between these cluster spawning potential and the natal origin proportions derived from the otolith geochemical analyses across all sampled locations. Pearson's coefficient r is 0.9912 with a p -value of 8.4664×10^{-2} for *D. sargus* and r is 0.9555 with a p -value of 7.8507×10^{-4} for *D. vulgaris* (Fig. 5c and d). Note that the largest number of natal origins for *D. vulgaris* provides a more robust correlation for *D. vulgaris* (indicated by its smaller p -value of 7.8507×10^{-4}) than for *D. sargus* (p -value of 8.4664×10^{-2}). When considering each sampling location independently, it is worth noting that the correlations still hold for both species, despite slightly larger spread (see SI B-8).

4. Discussion

4.1. Fitting modelled larval sources with otolith geochemistry to delineate and evaluate spawning areas

We delineate and evaluate the relative larval supplies of several discrete spawning areas by correlating simulated cluster spawning potential and observed natal origin proportions. By doing so, we confront a probabilistic model using millions of particle trajectories and an observational approach relying only on hundreds of otolith samples. The regression coefficients (i.e. the slope of the regression curve) are around 0,7 for both species, indicating that the model tends to overestimate the poorly represented natal origins and to underestimate the dominant ones (or the other way around, from the observational point-of-view). It suggests that the probabilistic approach is able to capture the larval sources of low probabilities, whereas the observational approach may have missed, or underrepresented, those weak sources since the corresponding post-settlers are rare and scattered in the field. Similarly, the dominant larval sources simulated by our model are one to two orders of magnitude more probable than the rare ones, indicating that the post-settlers sampled in the field have high probability to originate from these prominent sources and that the rare ones are likely to be missed. Ideally, and despite the arduous financial costs and efforts, field surveys should consider increasing the number of samples to apprehend properly those rare, yet ecologically important, sources. Our integrative approach shows great promises for the "a-priori" testing of different sampling strategies in order to provide scientifically-based guidance for the adequate spacing, sizing and sampling efforts of future field surveys. Despite difficulties owing to the large surfaces involved, further investigations could consist in surveying the discrete spawning

areas revealed here to observe, and eventually subsample, spawning aggregations of mature adults to validate our framework.

Notwithstanding the good agreement between cluster spawning potential and natal origin proportions, our empirical clustering procedure, which is based on expert knowledge, could be further generalized by using automatic and objective community detection algorithms (e.g. Rossi et al., 2014; Ser-Giacomi et al., 2015a). However, this is beyond the scope of the present manuscript due to the species- and sites-specific characteristics, the lack of information about seawater geochemistry (Di Franco et al., 2012b, 2015), along with the general opacity and inflexibility of most automatic clustering algorithms. Nonetheless, more precise and realistic characterization of spawning areas could be obtained through our empiric clustering methodology by incorporating additional information such as a geochemical atlas of seawater or supplementary connectivity knowledge inferred from genetic or tracking studies.

Despite these future developments, we present a general approach which allows to locate spawning areas and to better quantify larval connectivity patterns from pre-determined origins and destinations (Nolasco et al., 2018). In a context of sparse knowledge about fish spawning aggregations (Erisman et al., 2017), this information is critical for the management and conservation of marine ecosystems (see section 4.4). Furthermore, the existent published knowledge is rather biased toward tropical reef fishes (Russell et al., 2014). In this view, the present study complements recent research efforts (Calò et al., 2018) to improve our ability to locate spawning areas for temperate fish species inhabiting large and opened seascape.

4.2. Biological controls of connectivity

Our results evidence distinct scales of dispersion for both species, which are primarily due to specie-specific biological traits, namely the Pelagic Larval Duration (PLD, i.e. the time that larvae spend drifting in the ocean circulation). Indeed, *D. vulgaris*'s PLD is almost three times longer than *D. sargus*'s one, giving a ratio of ~ 2.8 which resemble most the mean ratio of their dispersal plume which reaches 4.1 ± 1.6 . In contrast, the mean ratio of *D. vulgaris* to *D. sargus*'s median dispersal distances is 0.9 ± 0.2 , while it is 1.7 ± 0.2 for the maximal distances. It suggests that dispersal distances and surfaces have very different relationship with the PLD, challenging the commonly accepted concept that PLD is a good predictor of dispersal (Shanks et al., 2003). We consider here only the median PLDs of both species to design our numerical experiments whereas the range of PLDs derived from otolith sclerochronology is indeed more extended (Di Franco and Guidetti, 2011; Di Franco et al., 2013). Previous findings suggest that considering more appropriately the full ranges of observed PLDs could return slightly different dispersal distances and surfaces. More specifically, the exact dispersal scales would theoretically be individual-specific since each larva (or each meter-scale larval patch) would follow a unique trajectory crossing various environmental conditions which can affect biological traits, including the PLD due to slower or faster development than average (Cowen and Sponaugle, 2009). However, since Monroy et al. (2017) showed that connectivity estimates for long PLDs are more robust against PLD uncertainties than for short PLDs, we expect some substantial influences of the extreme PLDs on the quantitative patterns of connectivity mainly for *D. sargus*.

From spawning to recruitment, the key factors controlling the connectivity of early-life stages are: (i) physically-driven larval transport processes, (ii) larval behavior potentially influencing the drift, (iii) substrate availability for settlement, and (iv) local biotic interactions among the post settlers (Pineda, 2000). The fine-tuning of the Lagrangian model parameters by data derived from otoliths of post-settled juveniles, which settled successfully and survived to local biotic interactions, allows to take factors (i), (iii) and (iv) into account in our

framework. Factor (ii) has not been explicitly accounted for here, while Sparidae larvae reared in the lab showed some swimming abilities toward the end of their ontogeny (Clark et al., 2005) and possibly orientating themselves via the position of the sun (Faillietaz et al., 2018). The assumption of passive larval drift was retained here because knowledge about species-specific larval behavior in the field are sparse and very uncertain. In addition, Nolasco et al. (2018) recently documented better correlations between connectivity observations and dispersal models simulating passive rather than active drift. Indeed, the diffusion applied to trajectories when adding random components to simulate active movements, as is commonly done, is of the same order of the numerical diffusion induced by the spatial discretization of the oceanic domain, including over the nearshore regions where swimming potential would be more probable (Rossi et al., 2014). Moreover, the sequential filtering reduces successively the dispersal distances that the passive assumption could have overestimated (Shanks, 2009). Although the early-life stages of most marine organisms, including coastal fishes, are thought to be the main drivers of dispersal, the active movements of adults and juveniles may also affect connectivity (Di Franco et al., 2015). Nevertheless, because juveniles have been sampled few days after settlement (Di Franco and Guidetti, 2011; Di Franco et al., 2013), that is before any significant post-settlement movements would occur, these processes do not affect our results. Last but not least, the overall contribution of adults to broad-scale dispersal can be reasonably neglected since these stages are rather territorial, especially littoral fishes that show strong site fidelity (Di Franco et al., 2018).

4.3. Hydrodynamical control of connectivity

Besides the biological control exerted on dispersal distances and surfaces discussed above, finer discrepancies of connectivity pathways and magnitudes are rather well-explained by the spatio-temporal variability of ocean currents. Larval sources found along Italian shorelines for both species are linked to the surface circulation of the Adriatic Sea (Artegiani et al., 1997a; Millot and Taupier-Letage, 2005). Most sources are located north-westward (i.e. upstream) of the sampled locations, which is in agreement with the dominant south-eastward alongshore transport related with the W-NAd, W-MAd and W-SAd currents (Carlson et al., 2016). Along the Apulian coast, source nodes with high probabilities are found close to the sampled locations, in line with Dubois et al. (2016) and Bray et al. (2017) who have already shown that the Apulian coast tends to act as a sink of larvae. Despite the presence of the W-SAd current transporting efficiently larvae south-eastward, prominent nearshore sources can be related to wind-induced coastal downwelling which prevails in this region during winter throughout to early spring (Artegiani et al., 1997b; Bakun and Agostini, 2001). Downwelling, and its associated coastal convergence, pushes larvae toward the coastline and increases retention there, leading to these high probabilities. This is consistent with Dubois et al. (2016) who showed that wind-driven convergent oceanic systems are usually characterized by larval sinks.

The coast-to-coast connections, linking both coastlines of the Adriatic Sea, is related to the sub-gyres cyclonic circulation (Carlson et al., 2016), namely the SAd and MAd gyres. While this finding has ecological and managerial implications (see section 4.4), these inter-coastal connections have a marginal contribution as compared to the sources spread along the Apulian shores, as suggested by Melià et al. (2016). Since the southern branch of the S-Ad gyre induces west-to-east connection (Carlson et al., 2016), the presence of larval sources on both sides of the Otranto strait for *D. vulgaris* would be rather due to the turbulent character of the local circulation, as evidenced by high eddy kinetic energy values (EKE, see SI B-2). Chaotic surface circulation could create intermittent but repeated pathways which allows inter-coastal

connectivity against the main direction of the current. In the same way, filaments of high EKE stretch out until the gulf of Taranto, allowing larval sources to be found there (Fig. 4b). Conversely, the narrower and intensified W-SAd jet-like current associated with low EKE off the Apulian coast in spring imply a directional connectivity with little cross-shore exchanges, explaining why only upstream well-aligned sources were captured for *D. sargus*, contrasting the more diffused and latitudinally-extended sources found for *D. vulgaris* in winter. In fact, while Lagrangian particles are here simulating passive larvae, they can also be seen as a finite fluid parcel. In this view, Ser-Giacomi et al. (2015a) found analytical relationships between diagnostics derived from the LFN connectivity matrices and finite-time Lyapunov exponent, which is a measure of local stretching properties in the ocean, as is EKE (Vaugh et al., 2006), hence supporting the link between purely physical variables and our connectivity diagnostics.

While a climatological description of the surface circulation explains well the differential connectivity of both species, it is evident that ocean currents exhibit in nature high levels of variability, including for longer time-scales such as inter-annual and inter-decadal ones. The oceanographic properties of the Adriatic Sea have been shown to respond to the Bimodal Oscillating system (BiOS) at decadal or shorter time-spans, which induces substantial inter-annual variability of its circulation (Mihanović et al., 2015). The dispersal patterns reported here would surely be impacted by such low-frequency variability, similarly to the strong inter-annuality of connectivity demonstrated in the north-west Mediterranean (Hidalgo et al., 2019). Note however that the BiOS has been related to large changes not only of hydrodynamics, which affect directly dispersal (Civitarese et al., 2010), but also of other abiotic factors such as temperature, which indirectly influences larval dispersal by modifying spawning behavior and larval traits (Green and Fisher, 2004). Analyzing inter-annuality of spawning is thus a complex task in which non-linear effects between several counter-acting processes may drive non-predictable results.

4.4. Exploiting connectivity information for conservation purposes

By delineating spawning areas and quantifying connectivity patterns which account for the spatio-temporal variability of ocean circulation and the spawning phenology, our framework provides information about when and where spawning aggregations could occur. Considering that many coastal fishes, including those of our case-studies, are exploited by small-scale (professional and recreational) fisheries, this is essential information for managers that is currently lacking (see section 4.1). It could constitute a sound scientific basis to improve fisheries management, for instance thanks to conservation plans that would specially target the discrete spawning areas, that is where putative spawning aggregations take place. The more abilities we have in appraising when and where spawning aggregation events occur, the more appropriate will be the dynamical and adaptative management measures (Heyman, 2014), hence favoring healthier local ecosystem and larval spillover to neighboring exploited areas (Erisman et al., 2017; Pelc et al., 2010). Indeed, small investments on well-placed and well-timed managerial constraints (e.g. seasonal closures, restricted no-take zone, etc) targeting spawning areas could lead to large benefits for fisheries, ecotourism and biodiversity conservation (Erisman et al., 2017).

In our case-studies, we showed that *D. vulgaris* Apulian subpopulation likely originate from several spawning areas located on both Adriatic shorelines. It suggests the need of a tight international collaboration between adjacent countries, e.g. Italy, Greece, Croatia and Albania, to ensure efficient fishery spatial management in the Adriatic Sea (Hidalgo et al., 2019; Ramesh et al., 2019). Among the total pool of larvae supplied to the Apulian coast, where professional and recreational fishing occurs, almost $\frac{1}{3}$ of *D. sargus* larvae and $\frac{1}{4}$ of *D. vulgaris*

larvae originated from the surrounding MPAs. Tremiti MPA emerges as the most important larval supplier of the studied stretch of coast: almost $\frac{1}{4}$ of *D. sargus* larvae and $\frac{1}{10}$ of *D. vulgaris* larvae settled in the Apulian coast likely originated from this MPA. Our model result, backed up by observation, clearly support the fact that an upgrade of Tremiti MPA enforcement level, currently under low enforcement (Guidetti et al., 2008), could cause significant benefit to *D. sargus* and *D. vulgaris* Apulian's populations. Then, using our findings to inform management (Erisman et al., 2017), we would recommend to strengthen conservation policies of Tremiti MPA.

Moreover, MPAs have positive effects on biomass and size distribution of larger fish (Lester et al., 2009), leading to an increase of their reproductive outputs. Indeed, MPAs could produce at least five times more offspring than same size unprotected areas (Marshall et al., 2019). Thanks to the flexibility of our model results, MPAs associated proportion (Fig. 4) could be scale up accordingly. Thus, all the MPAs (Tremiti MPA) would send almost $\frac{7}{10}$ ($\frac{6}{10}$) of *D. sargus* larvae and $\frac{6}{10}$ ($\frac{2}{10}$) of *D. vulgaris* larvae settled in the Apulian coast, highlighting dramatically the benefit of MPAs in the replenishment of Apulian coast. Providing such useful information is well aligned with the necessity to incorporate connectivity knowledge in conservation plans and MPAs design (Dubois et al., 2016; Balbar and Metaxas, 2019).

We also provide spatially-explicit and quantitative information to potentially implement new protection measures for the other non-protected regions identified here during the spawning seasons of each species. Indeed, our framework not only appraises the efficiency of the local MPAs network but also inform where and when additional measures could be implemented for the protection of spawning aggregations.

For both target fishes, our results evidence well-defined spawning areas, encompassing several spawning events occurring during a given year (e.g. spring 2009 for *D. sargus* and winter 2009–2010 for *D. vulgaris*), that are directly useable by stakeholders for that given year. What remain to be investigated however is how the geographical delimitation and relative contributions of these spawning regions vary from one year to another. As said in section 4.3, this non-trivial task is kept for future work since investigating properly the inter-annual variability of spawning areas requires the considerations of all biotic and abiotic factors (e.g. in addition of the ocean circulation) displaying inter-annual variations.

5. Conclusion

We proposed an integrative framework which combines Lagrangian particle modeling, network theory and published knowledge (encompassing otolith analyses, ecological and biogeographical information). It allows to locate precisely and assess spawning areas through an improved quantitative characterization of dispersal scales and connectivity patterns. Our multidisciplinary methodology is flexible as it can be readily adapted to any other case-study, providing a certain degree of knowledge about the fish species of interest. Biological traits such as the PLD and the spawning phenology (derived from otolith analyses), along with larval dispersal pathways imposed by the turbulent oceanic circulation (simulated by state-of-the-art Lagrangian modelling), shape together connectivity patterns and allow us to identify spawning areas, that are critical for adequate spatial conservation planning. We showed that our analytical approach is a powerful tool providing unprecedented information about spawning areas, which can be further refined as ocean circulation models gain in reliability and as connectivity knowledge from complementary observations increases. Furthermore, if the environmental (e.g. temperature, plankton) controls of spawning are well-known and considering the current development of forecasts by operational ocean models, our approach could even anticipate some

days ahead when and where spawning events are likely to occur, hence providing near-real time information for adaptive management and conservation plans.

Acknowledgment

V.R. thanks Prof. Paolo Guidetti for fruitful discussions. T.L. and V.R. acknowledge financial support from the European project SEAMoBB, funded by ERA-Net Mar-TERA and managed by ANR (number ANR_17-MART-0001_01). T.L. is supported by a PhD grant provided by the French government. A.D.F. and A.C. have been supported by the Safenet (funded by DG Mare) and FishMPABlue2 (co-financed by European Regional Development Fund-ERDF) projects. The project leading to this publication has received funding from European FEDER Fund under project 1166-39417. The authors thank two anonymous reviewers and the editor for their constructive comments that helped improve the original manuscript.

Appendix A. Supplementary data

Supplementary data to this article can be found online at <https://doi.org/10.1016/j.marenvres.2019.104761>.

References

- Alós, J., Cabanellas-Reboredo, M., March, D., 2012. Spatial and temporal patterns in the movement of adult two-banded sea bream *Diplodus vulgaris* (Saint-Hilaire, 1817). *Fish. Res.* 115, 82–88.
- Artegiani, A., Paschini, E., Russo, A., Bregant, D., Raicich, F., Pinardi, N., 1997a. The Adriatic Sea general circulation. Part I: air–sea interactions and water mass structure. *J. Phys. Oceanogr.* 27, 1492–1514.
- Artegiani, A., Paschini, E., Russo, A., Bregant, D., Raicich, F., Pinardi, N., 1997b. The Adriatic Sea general circulation. Part II: baroclinic circulation structure. *J. Phys. Oceanogr.* 27, 1515–1532.
- Aspillaga, E., Bartumeus, F., Linares, C., Starr, R.M., López-Sanz, J., Díaz, D., Zabala, M., Hereu, B., 2016. Ordinary and extraordinary movement behaviour of small resident fish within a Mediterranean marine protected area. *PLoS One* 11, e0159813.
- Bakun, A., Agostini, V.N., 2001. Seasonal patterns of wind-induced upwelling/downwelling in the Mediterranean Sea. *Sci. Mar.* 65, 243–257.
- Balbar, A.C., Metaxas, A., 2019. The current application of ecological connectivity in the design of marine protected areas. *Glob. Ecol. Conserv.* 17, e00569 <https://doi.org/10.1016/j.gecco.2019.e00569>, URL: <http://www.sciencedirect.com/science/article/pii/S2351989418304347>.
- Bray, L., Kassis, D., Hall-Spencer, J., 2017. Assessing larval connectivity for marine spatial planning in the Adriatic. *Mar. Environ. Res.* 125, 73–81. <https://doi.org/10.1016/j.marenvres.2017.01.006>, URL: <https://linkinghub.elsevier.com/retrieve/pii/S0141113617300430>.
- Burgess, S.C., Baskett, M.L., Grosberg, R.K., Morgan, S.G., Strathmann, R.R., 2016. When is dispersal for dispersal? Unifying marine and terrestrial perspectives. *Biol. Rev.* 91, 867–882. <https://doi.org/10.1111/brv.12198>, URL: <http://onlinelibrary.wiley.com/doi/abs/10.1111/brv.12198>.
- Calò, A., Félix-Hackradt, F.C., García, J., Hackradt, C.W., Rocklin, D., Treviño Otón, J., Charton, J.A.G., 2013. A review of methods to assess connectivity and dispersal between fish populations in the Mediterranean Sea. *Adv. Oceanogr. Limnol.* 4, 150–175.
- Calò, A., Lett, C., Mourre, B., Pérez-Ruzafa, J., García-Charton, J.A., 2018. Use of Lagrangian simulations to hindcast the geographical position of propagule release zones in a Mediterranean coastal fish. *Mar. Environ. Res.* 134, 16–27. <https://doi.org/10.1016/j.marenvres.2017.12.011>, URL: <https://linkinghub.elsevier.com/retrieve/pii/S0141113617305834>.
- Carlson, D.F., Griffa, A., Zambianchi, E., Suaria, G., Corgnati, L., Magaldi, M.G., Poulain, P.M., Russo, A., Bellomo, L., Mantovani, C., Celentano, P., Molcard, A., Borghini, M., 2016. Observed and modeled surface Lagrangian transport between coastal regions in the Adriatic Sea with implications for marine protected areas. *Cont. Shelf Res.* 118, 23–48. <https://doi.org/10.1016/j.csr.2016.02.012>, URL: <https://linkinghub.elsevier.com/retrieve/pii/S0278434316300620>.
- Ciannelli, L., Fisher, J., Skern-Mauritzen, M., Hunsicker, M., Hidalgo, M., Frank, K., Bailey, K., 2013. Theory, consequences and evidence of eroding population spatial structure in harvested marine fishes: a review. *Mar. Ecol. Prog. Ser.* 480, 227–243. <https://doi.org/10.3354/meps10067>, URL: <http://www.int-res.com/abstracts/meps/v480/p227-243/>.
- Ciliberti, S.A., Pinardi, N., Coppini, G., Oddo, P., Vukicevic, T., Lecci, R., Verri, G., Kumkar, Y., Creti, S., 2015. A high resolution Adriatic-Ionian Sea circulation model for operational forecasting. In: EGU General Assembly Conference Abstracts.
- Civitaresse, G., Gačić, M., Lipizer, M., Eusebi Borzelli, G.L., 2010. On the impact of the bimodal oscillating system (BIOS) on the biogeochemistry and biology of the adriatic

- and ionian seas (eastern mediterranean). *Biogeosciences* 7, 3987–3997, URL: <https://www.biogeosciences.net/7/3987/2010/bg-7-3987-2010.html> <https://doi.org/10.5194/bg-7-3987-2010>.
- Clark, D.L., Leis, J.M., Hay, A.C., Trnski, T., 2005. Swimming ontogeny of larvae of four temperate marine fishes. *Mar. Ecol. Prog. Ser.* 292, 287–300.
- Courant, R., Friedrichs, K., Lewy, H., 1928. Über die partiellen Differenzgleichungen der mathematischen Physik. *Math. Ann.* 100, 32–74. <https://doi.org/10.1007/BF01448839>, URL: <https://doi.org/10.1007/BF01448839>.
- Cowen, R.K., Paris, C.B., Srinivasan, A., 2006. Scaling of connectivity in marine populations. *Science* 311, 522–527.
- Cowen, R.K., Sponaugle, S., 2009. Larval Dispersal and Marine Population Connectivity.
- Di Franco, A., Calò, A., Pennetta, A., De Benedetto, G., Planes, S., Guidetti, P., 2015. Dispersal of larval and juvenile seabream: implications for Mediterranean marine protected areas. *Biol. Conserv.* 192, 361–368.
- Di Franco, A., Coppini, G., Pujolar, J.M., De Leo, G.A., Gatto, M., Lyubartsev, V., Melia, P., Zane, L., Guidetti, P., 2012a. Assessing dispersal patterns of fish propagules from an effective Mediterranean marine protected area. *PLoS One* 7, e52108.
- Di Franco, A., Gillanders, B.M., De Benedetto, G., Pennetta, A., De Leo, G.A., Guidetti, P., 2012b. Dispersal patterns of coastal fish: implications for designing networks of marine protected areas. *PLoS ONE* 7, e31681 <https://doi.org/10.1371/journal.pone.0031681>, URL: <http://dx.plos.org/10.1371/journal.pone.0031681>.
- Di Franco, A., Guidetti, P., 2011. Patterns of variability in early-life traits of fishes depend on spatial scale of analysis. *Biol. Lett.* 7, 454–456.
- Di Franco, A., Plass-Johnson, J.G., Di Lorenzo, M., Meola, B., Claudet, J., Gaines, S.D., García-Charton, J.A., Giakoumi, S., Grorud-Colvert, K., Hackrad, C.W., Micheli, F., Guidetti, P., 2018. Linking home ranges to protected area size: the case study of the Mediterranean Sea. *Biol. Conserv.* 221, 175–181. <https://doi.org/10.1016/j.biocon.2018.03.012>, URL: <http://www.sciencedirect.com/science/article/pii/S0006320717311187>.
- Di Franco, A., Qian, K., Calò, A., Di Lorenzo, M., Planes, S., Guidetti, P., 2013. Patterns of variability in early life traits of a Mediterranean coastal fish. *Mar. Ecol. Prog. Ser.* 476, 227–235.
- Di Lorenzo, M., D'Anna, G., Badalamenti, F., Giacalone, V.M., Starr, R.M., Guidetti, P., 2014. Fitting the size of no-take zones to species movement patterns: a case study on a Mediterranean seabream. *Mar. Ecol. Prog. Ser.* 502, 245–255.
- Domeier, M.L., Colin, P.L., 1997. Tropical reef fish spawning aggregations: defined and reviewed. *Bull. Mar. Sci.* 60, 698–726.
- Dubois, M., Rossi, V., Ser-Giacomi, E., Arnaud-Haond, S., López, C., Hernández-García, E., 2016. Linking basin-scale connectivity, oceanography and population dynamics for the conservation and management of marine ecosystems. *Glob. Ecol. Biogeogr.* 25, 503–515.
- Erisman, B., Heyman, W., Kobara, S., Ezer, T., Pittman, S., Aburto-Oropeza, O., Nemeth, R.S., 2017. Fish spawning aggregations: where well-placed management actions can yield big benefits for fisheries and conservation. *Fish Fish.* 18, 128–144. <https://doi.org/10.1111/faf.12132>, URL: <https://onlinelibrary.wiley.com/doi/abs/10.1111/faf.12132>.
- Faillietaz, R., Durand, E., Paris, C.B., Koubbi, P., Irsson, J.O., 2018. Swimming speeds of Mediterranean settlement-stage fish larvae nuance Hjort's aberrant drift hypothesis. *Limnol. Oceanogr.* 63, 509–523.
- Fortunato, S., 2010. Community detection in graphs. *Phys. Rep.* 486, 75–174.
- Fuiman, L.A., Connelly, T.L., Lowerre-Barbieri, S.K., McClelland, J.W., 2015. Egg boons: central components of marine fatty acid food webs. *Ecology* 96, 362–372. <https://doi.org/10.1890/14-0571.1>, URL: <https://esajournals.onlinelibrary.wiley.com/doi/abs/10.1890/14-0571.1>.
- Giacalone, V.M., Pipitone, C., Badalamenti, F., Sacco, F., Zenone, A., FERRERI, R., MICALE, V., BASILONE, G., D'ANNA, G., 2018. Home Range, Movements and Daily Activity of the White Seabream *Diplodus sargus* (Linnaeus, 1758) during the Spawning Season URL: <https://doi.org/10.21411/cbm.a.7c19e1b8> <http://application.sb-roscoff.fr/cbm/doi/10.21411/CBM.A.7C19E1B8>.
- Gibb, F.M., Régnier, T., Donald, K., Wright, P.J., 2017. Connectivity in the early life history of sandeel inferred from otolith microchemistry. *J. Sea Res.* 119, 8–16.
- Green, B.S., Fisher, R., 2004. Temperature influences swimming speed, growth and larval duration in coral reef fish larvae. *J. Exp. Mar. Biol. Ecol.* 299, 115–132. <https://doi.org/10.1016/j.jembe.2003.09.001>, URL: <http://www.sciencedirect.com/science/article/pii/S0022098103004404>.
- Guidetti, P., 2000. Differences among fish assemblages associated with nearshore Posidonia oceanica seagrass beds, rocky-algal reefs and unvegetated sand habitats in the Adriatic Sea. *Estuar. Coast Shelf Sci.* 50, 515–529.
- Guidetti, P., Milazzo, M., Bussotti, S., Molinari, A., Murenu, M., Pais, A., Spanò, N., Balzano, R., Agardy, T., Boero, F., Carrada, G., Cattaneo-Vietti, R., Cau, A., Chemello, R., Greco, S., Manganaro, A., Notarbartolo di Sciarra, G., Russo, G.F., Tunesi, L., 2008. Italian marine reserve effectiveness: does enforcement matter? *Biol. Conserv.* 141, 699–709. <https://doi.org/10.1016/j.biocon.2007.12.013>, URL: <http://www.sciencedirect.com/science/article/pii/S0006320707004685>.
- Harmelin-Vivien, M., Harmelin, J., Leboulloux, V., 1995. Microhabitat requirements for settlement of juvenile sparid fishes on Mediterranean rocky shores. *Hydrobiologia* 300, 309–320.
- Heithaus, M.R., Frid, A., Wirsing, A.J., Worm, B., 2008. Predicting ecological consequences of marine top predator declines. *Trends Ecol. Evol.* 23, 202–210. <https://doi.org/10.1016/j.tree.2008.01.003>, URL: <http://www.sciencedirect.com/science/article/pii/S0169534708000578>.
- Henry, L.A., Mayorga-Adame, C.G., Fox, A.D., Polton, J.A., Ferris, J.S., McLellan, F., McCabe, C., Kutti, T., Roberts, J.M., 2018. Ocean sprawl facilitates dispersal and connectivity of protected species. *Sci. Rep.* 8, 11346. <https://doi.org/10.1038/s41598-018-29575-4>, URL: <http://www.nature.com/articles/s41598-018-29575-4>.
- Heyman, W.D., 2014. Let Them Come to You: Reinventing Management of the Snapper-Grouper Complex in the Western Atlantic: A Contribution to the Data Poor Fisheries Management Symposium, vol. 7.
- Hidalgo, M., Rossi, V., Monroy, P., Ser-Giacomi, E., Hernández-García, E., Guijarro, B., Massutí, E., Alemany, F., Jadaud, A., Perez, J.L., Reglero, P., 2019. Accounting for ocean connectivity and hydroclimate in fish recruitment fluctuations within trans-boundary metapopulations. *Ecological Applications* 0, e01913 <https://doi.org/10.1002/eap.1913>, URL: <http://esajournals.onlinelibrary.wiley.com/doi/abs/10.1002/eap.1913>.
- Kingsford, M.J., 1988. The early life history of fish in coastal waters of northern New Zealand: a review. *N. Z. J. Mar. Freshw. Res.* 22, 463–479. <https://doi.org/10.1080/00288330.1988.9516316>, URL: <https://doi.org/10.1080/00288330.1988.9516316>.
- Kool, J.T., Moilanen, A., Trem, E.A., 2013. Population connectivity: recent advances and new perspectives. *Landsc. Ecol.* 28, 165–185.
- Lenfant, P., Planes, S., 1996. Genetic differentiation of white sea bream within the Lion's gulf and the Ligurian sea (Mediterranean Sea). *J. Fish Biol.* 49, 613–621.
- Lester, S.E., Halpern, B.S., Grorud-Colvert, K., Lubchenco, J., Ruttenberg, B.I., Gaines, S.D., Airamé, S., Warner, R.R., 2009. Biological effects within no-take marine reserves: a global synthesis. *Mar. Ecol. Prog. Ser.* 384, 33–46.
- Levin, P.S., 1994. Fine-scale temporal variation in recruitment of a temperate demersal fish: the importance of settlement versus post-settlement loss. *Oecologia* 97, 124–133. <https://doi.org/10.1007/BF00317916>, URL: <https://doi.org/10.1007/BF00317916>.
- Lowe, W.H., Kovach, R.P., Allendorf, F.W., 2017. Population genetics and demography unite ecology and evolution. *Trends Ecol. Evol.* 32, 141–152. <https://doi.org/10.1016/j.tree.2016.12.002>, URL: [https://www.cell.com/trends/ecology-evolution/abstract/S0169-5347\(16\)30235-X](https://www.cell.com/trends/ecology-evolution/abstract/S0169-5347(16)30235-X).
- Madeç, G., others, 2015. NEMO Ocean Engine.
- Marshall, D.J., Gaines, S., Warner, R., Barneche, D.R., Bode, M., 2019. Underestimating the benefits of marine protected areas for the replenishment of fished populations. *Front. Ecol. Environ.* <https://doi.org/10.1002/fee.2075>, URL: <http://esajournals.onlinelibrary.wiley.com/doi/abs/10.1002/fee.2075>.
- Melià, P., Schiavina, M., Rossetto, M., Gatto, M., Frascchetti, S., Casagrandi, R., 2016. Looking for hotspots of marine metacommunity connectivity: a methodological framework. *Sci. Rep.* 6, 23705.
- Mihanović, H., Viličić, I., Dunić, N., Šepić, J., 2015. Mapping of decadal middle Adriatic oceanographic variability and its relation to the BIOS regime: MAPPING OF DECADEAL ADRIATIC VARIABILITY. *J. Geophys. Res. Oceans* 120, 5615–5630. <https://doi.org/10.1002/2015JC010725>, URL: <http://doi.wiley.com/10.1002/2015JC010725>.
- Millot, C., Taupier-Letage, I., 2005. Circulation in the Mediterranean Sea. In: *The Mediterranean Sea*. Springer, pp. 29–66.
- Mitcheson, Y.S.d., Craig, M.T., Bertocini, A.A., Carpenter, K.E., Cheung, W.W.L., Choat, J.H., Cornish, A.S., Fennessy, S.T., Ferreira, B.P., Heemstra, P.C., Liu, M., Myers, R.F., Pollard, D.A., Rhodes, L.A., Rocha, L.A., Russell, B.C., Samoilys, M.A., Sanciangco, J., 2013. Fishing groupers towards extinction: a global assessment of threats and extinction risks in a billion dollar fishery. *Fish Fish.* 14, 119–136. <https://doi.org/10.1111/j.1467-2979.2011.00455.x>, URL: <http://onlinelibrary.wiley.com/doi/abs/10.1111/j.1467-2979.2011.00455.x>.
- Monroy, P., Rossi, V., Ser-Giacomi, E., López, C., Hernández-García, E., 2017. Sensitivity and robustness of larval connectivity diagnostics obtained from Lagrangian Flow Networks. *ICES (Int. Counc. Explor. Sea) J. Mar. Sci.* 74, 1763–1779.
- Nolasco, R., Gomes, I., Peteiro, L., Albuquerque, R., Luna, T., Dubert, J., Swearer, S.E., Queiroga, H., 2018. Independent estimates of marine population connectivity are more concordant when accounting for uncertainties in larval origins. *Sci. Rep.* 8, 2641. <https://doi.org/10.1038/s41598-018-19833-w>, URL: <http://www.nature.com/articles/s41598-018-19833-w>.
- Oddo, P., Pinardi, N., Zavatarelli, M., Coluccelli, A., 2006. The Adriatic basin forecasting system. *Acta Adriat. Int. J. Mar. Sci.* 47, 169–184.
- Olivar, M., Sabatés, A., 1997. Vertical distribution of fish larvae in the north-west Mediterranean Sea in spring. *Mar. Biol.* 129, 289–300.
- Pelc, R.A., Warner, R.R., Gaines, S.D., Paris, C.B., 2010. Detecting larval export from marine reserves. *Proc. Natl. Acad. Sci.* 107, 18266–18271. <https://doi.org/10.1073/pnas.0907368107>, URL: <https://www.pnas.org/content/107/43/18266>.
- Pineda, J., 2000. Linking larval settlement to larval transport: assumptions, potentials, and pitfalls. *Oceanogr. East. Pac.* 1, 84–105.
- Pineda, J., Hare, J.A., Sponaugle, S., 2007. Larval transport and dispersal in the coastal ocean and consequences for population connectivity. *Oceanography* 20, 22–39.
- Pujolar, J.M., Schiavina, M., Di Franco, A., Melià, P., Guidetti, P., Gatto, M., De Leo, G.A., Zane, L., 2013. Understanding the effectiveness of marine protected areas using genetic connectivity patterns and Lagrangian simulations. *Divers. Distrib.* 19, 1531–1542.
- Ramesh, N., Rising, J.A., Oremus, K.L., 2019. The small world of global marine fisheries: the cross-boundary consequences of larval dispersal. *Science* 364, 1192–1196. <https://doi.org/10.1126/science.aav3409>, URL: <https://science.sciencemag.org/content/364/6446/1192>.
- Richards, W.J., Lindeman, K.C., 1987. Recruitment dynamics of reef fishes: planktonic processes, settlement and demersal ecologies, and fishery analysis. *Bull. Mar. Sci.* 41, 392–410.
- Rossi, V., Ser-Giacomi, E., López, C., Hernández-García, E., 2014. Hydrodynamic provinces and oceanic connectivity from a transport network help designing marine reserves. *Geophys. Res. Lett.* 41, 2883–2891.

- Russell, M.W., de Mitcheson, Y.S., Erisman, B.E., Hamilton, R.J., Luckhurst, B.E., Nemeth, R.S., 2014. Status Report World's Fish Aggregations 2014. 13.
- Sadovy, Y., Domeier, M., 2005. Are aggregation-fisheries sustainable? Reef fish fisheries as a case study. *Coral Reefs* 24, 254–262. <https://doi.org/10.1007/s00338-005-0474-6>, URL: <http://link.springer.com/10.1007/s00338-005-0474-6>.
- Ser-Giacomi, E., Rodríguez-Méndez, V., López, C., Hernández-García, E., 2017. Lagrangian Flow Network approach to an open flow model. *Eur. Phys. J. Spec. Top.* 226, 2057–2068. <https://doi.org/10.1140/epjst/e2017-70044-2>, URL: <https://doi.org/10.1140/epjst/e2017-70044-2>.
- Ser-Giacomi, E., Rossi, V., López, C., Hernandez-García, E., 2015a. Flow networks: a characterization of geophysical fluid transport. *Chaos. Interdiscip. J. Nonlinear Sci.* 25, 036404.
- Ser-Giacomi, E., Vasile, R., Hernandez-García, E., Lopez, C., 2015b. Most probable paths in temporal weighted networks: an application to ocean transport. *Physical Review E* 92. <https://doi.org/10.1103/PhysRevE.92.012818>. arXiv: 1411.6902, URL: <http://arxiv.org/abs/1411.6902>.
- Shanks, A.L., 2009. Pelagic larval duration and dispersal distance revisited. *Biol. Bull.* 216, 373–385. <https://doi.org/10.1086/BBLv216n3p373>, URL: <https://www.journals.uchicago.edu/doi/10.1086/BBLv216n3p373>.
- Shanks, A.L., Grantham, B.A., Carr, M.H., 2003. Propagule dispersal distance and the size and spacing of marine reserves. *Ecol. Appl.* S159–S169.
- Thresher, R.E., Colin, P.L., Bell, L.J., 1989. Planktonic duration, distribution and population structure of western and central pacific damselfishes (pomacentridae). *Copeia* 1989 420–434. <https://doi.org/10.2307/1445439>, URL: <https://www.jstor.org/stable/1445439>.
- Waugh, D.W., Abraham, E.R., Bowen, M.M., 2006. Spatial variations of stirring in the surface ocean: a case study of the Tasman Sea. *J. Phys. Oceanogr.* 36, 526–542.

UNCORRECTED PROOF